

---

## Research Paper

---

# Nanoparticles of Poorly Water-Soluble Drugs Prepared by Supercritical Fluid Extraction of Emulsions

Boris Y. Shekunov,<sup>1,2</sup> Pratibhash Chattopadhyay,<sup>1</sup> Jeff Seitzinger,<sup>1</sup> and Robert Huff<sup>1</sup>

Received May 17, 2005; accepted September 20, 2005

**Purpose.** The aim of the study was to develop and evaluate a new method for the production of micro- and nanoparticles of poorly soluble drugs for drug delivery applications.

**Methods.** Fine particles of model compounds cholesterol acetate (CA), griseofulvin (GF), and megestrol acetate (MA) were produced by extraction of the internal phase of oil-in-water emulsions using supercritical carbon dioxide. The particles were obtained both in a batch or a continuous manner in the form of aqueous nanosuspensions. Precipitation of CA nanoparticles was used for conducting a mechanistic study on particle size control and scale-up. GF and MA nanoparticles were produced in several batches to compare their dissolution behavior with that of micronized materials. The physical analysis of the particles produced was performed using dynamic light scattering (particle size), scanning electron microscopy (morphology), powder X-ray diffraction (crystallinity), gas chromatography (residual solvent), and a dissolution apparatus.

**Results.** Particles with mean volume diameter ranging between 100 and 1000 nm were consistently produced. The emulsion droplet size, drug solution concentration, and organic solvent content in the emulsion were the major parameters responsible for particle size control. Efficient and fast extraction, down to low parts-per-million levels, was achieved with supercritical CO<sub>2</sub>. The GF and MA nanoparticles produced were crystalline in nature and exhibited a 5- to 10-fold increase in the dissolution rate compared with that of micronized powders. Theoretical calculations indicated that this dissolution was governed mainly by the surface kinetic coefficient and the specific surface area of the particles produced. It was observed that the necessary condition for a reliable and scalable process was the sufficient emulsion stability during the extraction time.

**Conclusion.** The method developed offers a viable alternative to both the milling and constructive nanoparticle formation processes. Although preparation of a stable emulsion can be a challenge for some drug molecules, the new technique significantly shortens the processing time and overcomes the current limitations of the conventional precipitation techniques in terms of large waste streams, product purity, and process scale-up.

**KEY WORDS:** drug bioavailability; emulsions; nanoparticles; supercritical fluids.

## INTRODUCTION

Many of the new drug molecules are considered bio-pharmaceutical class II—low solubility and high permeability. Administration of such drugs presents a significant challenge because of their low bioavailability, high toxicity, and irregular absorption in the gastrointestinal tract. An effective way of alleviating these challenges is by reducing these materials into nanoparticles with enhanced dissolution rates because of increased surface area and chemical potential (1). Comminution of poorly water-soluble drugs into nanoparticles represents a very general approach to drug solubiliza-

tion because it requires no use of specific solubilizing excipients and, in addition, can be suitable not only for oral delivery but also for respiratory, injectable, and topical administration (2–4). Production of nanoparticulate powders or suspensions is a relatively new area of pharmaceutical technology and therefore requires a careful assessment of the product consistency, process robustness, and scalability.

Current approaches for production of nanoparticles fall into two major categories: particle size reduction by micronization and direct particle formation. Micronization is typically accomplished by wet milling (4,5) or high-pressure homogenization (3,6). Although commercially proven and widely used, these techniques may exhibit several shortcomings, e.g., difficulty to reduce the size below certain limits for ductile organic pharmaceuticals, possible contamination with grinding media, and/or adverse effects of the high shear and temperatures on the chemical and physical stability of

---

<sup>1</sup> Posnick Center of Innovative Technology, Ferro Corporation, Independence, Ohio 44131, USA.

<sup>2</sup> To whom correspondence should be addressed. (e-mail: shekunovb@ferro.com)

the materials (7). “Constructive” methods of the direct nanoparticle formation include solution precipitation with stabilizers (8,9), supercritical fluid (SCF) precipitation (10–12), and emulsion-based particle formation (13–15). The challenge of particle size control in all precipitation methods is that most small-molecular drugs tend to form relatively large crystals. This is because of a competition between nucleation and growth mechanisms, which typically result in the particles within 10- to 100- $\mu\text{m}$  size range, even under ideal mixing conditions (16). To decrease the mean particle size, high concentrations of growth blocking or “stabilizing” excipients are usually required (8). These growth inhibitors must be compound-specific. Unfortunately, commonly used pharmaceutical excipients such as polysorbate (Tween), polyvinyl pyrrolidone (PVP), polyvinyl alcohol (PVA), or hydroxymethylcellulose may not be efficient enough in interacting with crystal surfaces. Furthermore, the use of “tailor-made” additives, molecularly designed to inhibit crystal growth, is restricted very much because of the purity control and toxicity issues. The use of SCF in recent years facilitates fast precipitation and, importantly, enables the production of pure dry powders in a single step (17,18). However, the production of submicron particles is still very challenging here because of the same general limitations of the crystallization–precipitation mechanism (11). Being very material-specific, SCF precipitation of the crystalline materials typically results in particles within the lower-micron size range 1–10  $\mu\text{m}$ .

Compared to the direct precipitation, oil-in-water (o/w) emulsions can offer an enhanced particle size reduction and more flexibility in achieving some specific objectives, e.g., shape, crystallinity, and surface properties. Particle formation in emulsions is usually achieved by removal of the internal organic–oil phase, containing the water-insoluble drug, from the emulsion droplets either by solvent extraction, evaporation, or diffusion (1,13–15). Although these emulsion techniques are widely used on the laboratory scale, large-scale production presents many development hurdles, in particular, emulsion instability during processing, high residual solvent concentrations in the product, and long processing times. Inefficiency of mass-transfer mechanism in emulsion may also lead to inconsistency of particle size distribution, crystal growth or “ripening,” and agglomeration, making the scale-up difficult.

This work presents a new method, supercritical fluid extraction of emulsions (SFEE), which combines the flexibility of particle engineering using different emulsion systems with the efficiency of large-scale, continuous extraction with SCF. The process is based on the extraction of o/w emulsions using supercritical carbon dioxide. The major objectives of the present study are to show the feasibility of producing particulates with enhanced dissolution rate, to investigate the mechanism of particle formation, and, finally, to show the applicability of the continuous scale-up approach for this nanoparticle production. The model materials selected for this study composed of the following: cholesterol acetate (CA)—chosen because its structure is analogous to the backbone of many steroids; megestrol acetate (MA)—a well-known compound that exhibits problems with mechanical micronization; and, finally, griseofulvin (GF)—a water-insoluble antifungal agent chosen as a model drug because of its persistent acicular morphology and difficulties in size reduction using SCF precipitation techniques.

## MATERIALS AND METHODS

### Chemicals

All of the following materials were used as received:  $\text{CO}_2$  (99.9% pure, AGA), deionized water (99.9% pure, Aldrich Chemical Co., Milwaukee, WI, USA), PVA (mol. wt. 30,000–55,000, Aldrich Chemical Co.), pluronic F68 and F128 (BASF Corp., Worcester, MA, USA), Span 80 (Aldrich Chemical Co.), Tween 80 (Aldrich Chemical Co.), ethyl acetate [EA, 99.9% pure high-performance liquid chromatography (HPLC) grade, Aldrich Chemical Co.], toluene (99.9% pure HPLC grade, Aldrich Chemical Co.), dichloromethane (DCM, 99.9% pure HPLC grade, Aldrich Chemical Co.), GF (Sigma-Aldrich Co., Deisenhofen, Germany), MA (Sigma-Aldrich Co.), CA (Sigma-Aldrich Co.), and phosphate buffer (pH 7.4, Fisher Scientific, Fair Lawn, NJ, USA).

### Preparation of Emulsions

Model drugs were dissolved into suitable water-saturated organic solvents (EA, toluene, or DCM) to form a solution with concentration between 1 and 5% w/w. This solution was then dispersed into solvent-saturated aqueous solution of the surfactant (PVA, pluronics, lecithin, Span 80, or Tween 80) to form a crude emulsion (10–30% w/w organic phase) and subjected to high-pressure homogenization using a Microfluidizer (Microfluidics Inc., Newton, MA, USA) at 15–18 kpsi and three passes to form a fine emulsion with a mean droplet size between 200 and 1000 nm.

### Extraction Process

A schematic representation of the continuous system, designed for a pilot production scale, is shown in Fig. 1. The extraction of emulsions and particle precipitation was carried out in an electrically heated stainless-steel extraction column (1.5 m long, 4-l volume). The SCF fluid delivery system consisted of a liquid  $\text{CO}_2$  pump (P-200, Thar Technologies, Inc., Pittsburgh, PA, USA) and a heat exchanger, which provided SC  $\text{CO}_2$  to the bottom of the extraction column through a 0.5- $\mu\text{m}$  frit at flow rates up to 200 g/min. This frit maximized the mass-transfer efficiency during extraction. The emulsion was delivered from the top countercurrently using a semipreparative HPLC pump PU-2086 (Jasco Inc., Tokyo, Japan) supplying up to 20-ml/min constant flow rate. The emulsion was injected through a 150- $\mu\text{m}$  nozzle, which broke the emulsion into droplets, thereby increasing its surface area of contact with SC  $\text{CO}_2$ . The ratio between the flow rates of the SC  $\text{CO}_2$  and the emulsion was maintained constant, typically at 10:1. No static mixing elements inside the column were used in these experiments. The aqueous suspension formed was collected at the bottom of the column and continuously removed through a needle valve. The effluent SC  $\text{CO}_2$  was vented from the top of the column. The pressure inside the column was maintained constant using a backpressure regulator valve (Tescom Inc., Sunnyvale, CA, USA). The extraction temperature and pressure were maintained constant at 35°C and 80 bar correspondingly unless specified otherwise.

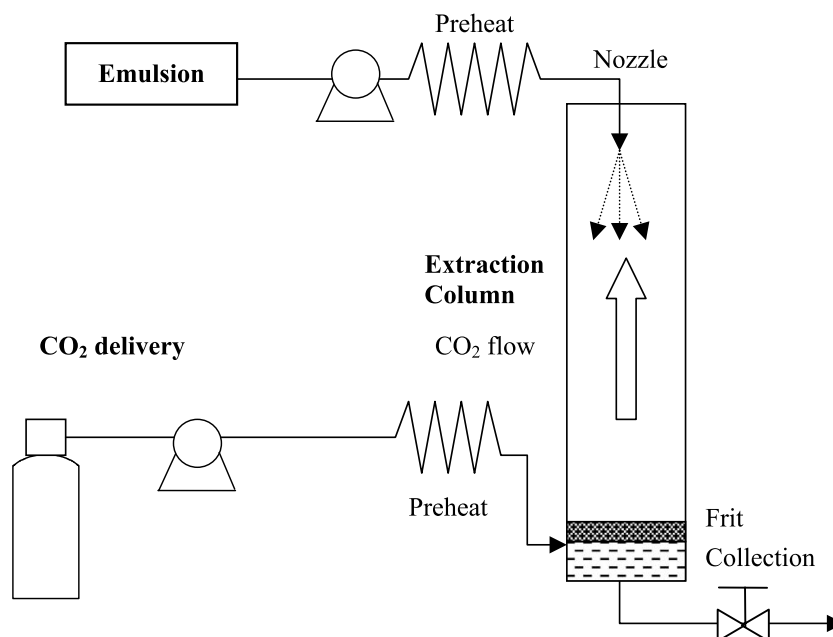


Fig. 1. Schematic of the continuous, 4-l extraction column process.

The batch apparatus used was similar to the continuous configuration, but included a smaller, 25-ml-volume, extraction column connected to a UV-vis detector (MD-1510, Jasco Inc.) to monitor the amount of solvent extracted from the emulsion. Carbon dioxide, delivered by a PU-1580-CO<sub>2</sub> pump (Jasco Inc.), was bubbled into the cell at constant flow rate, between 1 and 5 g/min. The extraction temperature was maintained constant at 35°C within an air-heated oven CO-1560 (Jasco Inc.). The backpressure regulator BP-1580-81 (Jasco Inc.) maintained a constant working pressure (80 bar) during the run. After the extraction process was complete, the suspension was removed for analysis and further processing.

### Residual Solvent in Suspension

The efficiency of solvent removal from the emulsion during extraction using SC CO<sub>2</sub> was determined by performing the experiments using the continuous SFEE apparatus (Fig. 1). Ethyl acetate in water emulsions was introduced into the extraction column, maintained at a pressure between 80 and 200 bar and a temperature between 35 and 80°C, at emulsion flow rates ranging between 1 and 10 ml/min. The product from the extraction column was collected at regular time intervals and analyzed for the residual ethyl acetate content using gas chromatography (GC). GC was carried out using a 6890 apparatus (Agilent, Wilmington, DE, USA) and DB-624 column (J&W Scientific, Folsom, CA, USA), a 75 m × 0.53 mm, 3-μm film column, at He flow rate of 40 cm/s. An inlet temperature of 150°C was employed. The oven temperature was increased from 40 to 100°C at 10°C/min. A flame ionization detector was used at 250°C.

### Drug Content in Suspension

All nanoparticles in the aqueous suspensions were first dissolved in a known amount of a suitable solvent (e.g.,

acetonitrile) to form a clear solution. The total drug content in the suspension was obtained by HPLC analysis of this clear solution. The aqueous suspensions were also filtered through a 0.02-μm syringe filter (Millipore Inc., Bedford, MA, USA). The dissolved drug content in the suspension was obtained by analyzing the filtrate with HPLC (Waters, Milford, MA, USA). The solid content was obtained by subtracting the drug content in the filtrate from the total drug content in the aqueous suspension. A 3.9 × 150-mm, 4-μm, Synergi MAX-RP column (Phenomenex, Torrance, CA, USA) was used for analysis. The column temperature was set at 30°C. For MA analysis, a mobile phase of acetonitrile/water (90:10, v/v) was used and delivered at a flow rate of 1.0 ml/min. The injection volume was 10 μl, and the retention time was 2.7 min. For GF analysis, a mobile phase of water/acetonitrile/tetrahydrofuran (60:35:5, v/v) was used and delivered at a flow rate of 1.5 ml/min. The injection volume was 10 μl, and the retention time was 4.9 min.

### Solid Samples Preparation

Excess water with surfactant from the suspensions was removed by high-speed centrifugation (Damon/TEC HT Centrifuge, Ramsey, MN, USA) followed by decantation. Centrifugation was carried out at 12,000–14,000 rpm for 10 min and was repeated twice to achieve maximum surfactant removal. The wet paste obtained was frozen at -20°C and lyophilized using a freeze dry system Feezone 4.5 (Labconco Co, Kansas City, MS, USA).

### Particle Size and Morphology

Scanning electron microscope (SEM; Amray 3300 FE) was used for image analysis. The powders were placed onto an aluminum stub and coated with gold/palladium using a sputter coater (Cressington 208HR). The mean particle sizes

of starting micronized reference materials (GF and MA) were obtained using Model 3603 Particle Size Distribution Analyzer (TSI, St. Paul, MN, USA), and these results were also correlated with the SEM results.

A dynamic light scattering instrument (DLS, PSS Nicomp 380, Santa Barbara, CA, USA) was used to determine the hydrodynamic number-weighted mean diameter (NMD) and volume-weighted diameter (VMD) of the nanoparticles in suspension and also to measure the corresponding mean diameters of the emulsions prepared. The optical concentration in the measuring cell was adjusted by dilution with deionized water. Each sample was run for 10 min.

### Drug Crystallinity

X-ray diffraction samples were prepared either by back-packing in aluminum frames or by placing them on a zero-background plate (quartz cut off the angle). The instrument used was a Philips XRG3100 generator using APD3720 software. The samples were run at 40 kV and 30 mA using Cu radiation. A monochromator was used along with a fixed divergence slit of 1°. A step size of 0.015° for 1 s was utilized. The 2 $\theta$  scanning range was between 5° and 40°.

### Dissolution Tests

Dissolution experiments were carried out using a dissolution bath and steerer similar to those of the USP Apparatus 2. The dissolution medium used was 100 ml of pH 7.4 phosphate buffer solution, which was incubated in a water bath at 37°C. A known amount of the aqueous suspension of drug nanoparticles or the starting material was introduced into the dissolution media at constant stirring. Approximately 1-ml

samples were collected from the dissolution media at regular time intervals, filtered through a 0.02- $\mu$ m syringe filter and analyzed by the HPLC method described above. Sink conditions were maintained throughout the dissolution testing period. All dissolution experiments were performed in duplicates, and all sample analyses were carried out in triplicates.

## RESULTS

### Particle Formation of Cholesterol Acetate and Solvent Extraction Efficiency

Figure 2 shows dependence of the CA particle size on the concentration of both EA and CA in the emulsion. The particle size reduction was observed with decrease of the solvent content and with decrease of the drug concentration. Figure 3 shows the SEM micrographs of the processed material and a typical size distribution curve of the CA nanoparticles. All batches showed a relatively narrow size distribution. Importantly, this size distribution is achieved in the suspension as “processed” without undergoing any

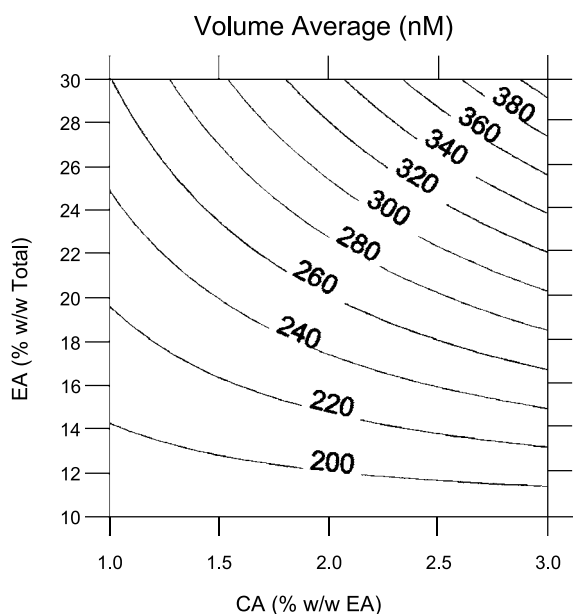


**Fig. 2.** Volume mean diameter of cholesterol acetate (CA) particles as a function of solution concentration and solvent content of the internal emulsion phase; the data are plotted as response surfaces according to an interaction model.

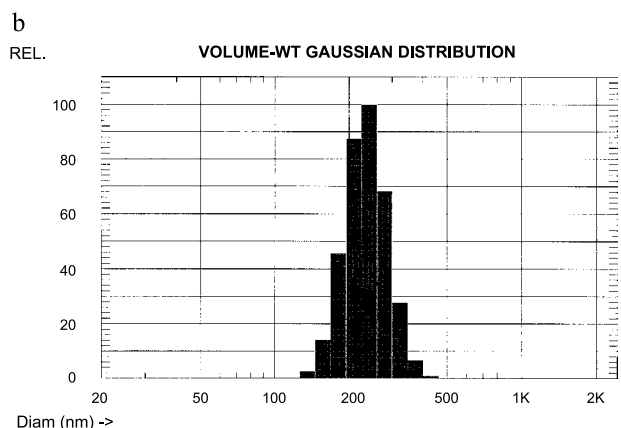
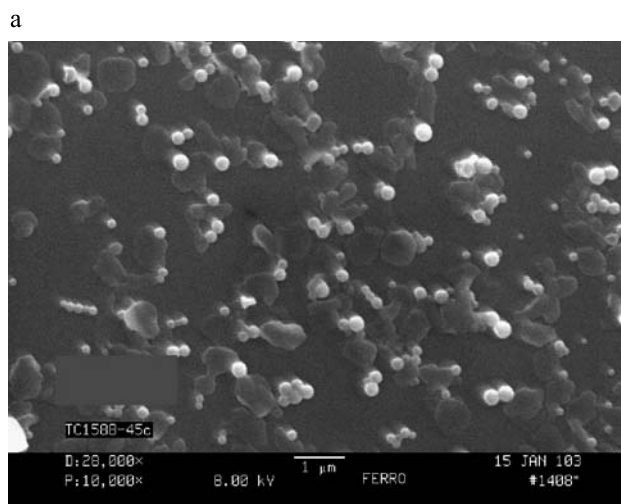


**Fig. 3.** Cholesterol acetate particles produced using supercritical fluid extraction of emulsions (SFEE) method: (a) morphology—some PVA precipitated from the suspension is also visible and (b) the corresponding particle size distribution by dynamic light scattering.

**Table I.** Concentration of the Unextracted Organic Phase in the Aqueous Suspension at Different Process Conditions

Pressure (bar)	Solution flow rate (ml/min)	Temperature (°C)	CO <sub>2</sub> flow rate (g/min)	Concentration (ppm)
80	1	35	10	47.8
80	1	35	50	54
80	5.5	35	30	9
140	1	35	30	12
200	1	35	30	0
200	10	35	10	11
80	1	67.5	30	11

further treatment such as filtration, deagglomeration, etc. CA nanoparticles formed stable aqueous dispersions. After 3 months of storage at room temperature, some partial sedimentation was observed. However, uniform nanosuspensions were obtained again upon light shaking. There was negligible change (<5%) in the mean volume diameter of particles, indicating no significant particle growth or agglomeration.

The process scale-up was investigated from the batch to continuous method. This scale-up corresponded to about 1:100 both by the rate of production and processing volume. The particles obtained using the same emulsion had the size distribution within 10% standard deviation.

The efficiency of the solvent extraction in the continuous SFEE, as a function of pressure, temperature, and flow rates, is shown in Table I. Within similar residence times (i.e., time required for the emulsion to pass through the column), the solvent extraction was found to be more efficient with increase of pressure and was practically independent of the solution flow rate under the conditions investigated.

### Production of Megestrol Acetate and Griseofulvin Suspensions

The experimental data obtained for MA samples produced in the batch mode are shown in Table II. The goal of these experiments was to show the feasibility of extraction of a high-boiling, nonvolatile organic solvent phase, such as toluene, and also to investigate the effect of the emulsion composition and the MA solution concentration on the particle size produced. It was observed, very similar to the CA, that there was a decrease in the particle size with decrease in the organic phase fraction of emulsions. Toluene was successfully removed from these emulsions to concentrations below 20-ppm level.

Precipitation of GF nanoparticles was carried out using the continuous mode precipitation method as shown in

Table III. Figure 4 represents the photographs of the larger particles obtained using SFEE (Fig. 4a), whereas the particles in Fig. 4b were produced using a supercritical antisolvent (SAS) precipitation technique according to the method described in another study (18). The pressure, temperature, and solution flow rate were selected the same for both the SFEE and SAS methods, and therefore, these experiments are representative of the different mechanism of particle formation afforded by supercritical fluid extraction and precipitation, respectively. Substantial difference is observed in the particle size and shape. It is very characteristic for the SAS process to attain the acicular morphology of GF with longest crystal dimensions between 20 and 200  $\mu\text{m}$  and VMD above 10  $\mu\text{m}$ . In contrast, the SFEE produced prismatic crystals with VMD typically between 0.5 and 1  $\mu\text{m}$  (Table III). Thus, the 10-fold reduction in the particle size and the production of uniform nonagglomerated GF particles with a small aspect ratio were achieved using SFEE. In all cases, the particles produced were crystalline, according to X-ray diffraction (XRD) and also as clearly seen from the faceted morphology of particles in Fig. 4a.

### Dissolution Behaviour of Nanosuspensions

Jet-milled MA, used as a reference material, consisted of crystalline microparticles with VMD = 2.9  $\mu\text{m}$  (Table II). GF with characteristic VMD = 5.9  $\mu\text{m}$  showed a typical “halo” in the XRD scan, indicating that this was an amorphous compound. Figure 5 shows that the nanosuspensions of MA have enhanced dissolution rate by a factor of 4 during the first 10 min, with nearly 100% of the drug dissolved during this period. The dissolution rate for the GF suspensions (Fig. 6) depended on the particle size. It was increased by factors 2 and 4 during the first 4 min for VMD = 980 and 760 nm, respectively, compared with the reference. Nearly 100% of the drug was dissolved within a period of 8 min. It is

**Table II.** Volume- and Number-Weighted Mean Diameters (VMD and NMD) and Corresponding Standard Deviations (SD) of Megestrol Acetate (MA) Particles Obtained Using the Batch Supercritical Fluid Extraction of Emulsions (SFEE) Method in Relationship to the Solvent Phase and Drug Concentration

MA (% w/w)	Solvent (toluene) (% w/w)	Surfactant (% w/w water)	VMD (SD) (nm)	NMD (SD) (nm)
1	20	Tween-80/0.4	192 (91)	69 (32)
1	30	Tween-80/0.4	254 (76)	174 (52)
2	20	Tween-80/0.4	180 (89)	60 (28)
2	30	Tween-80/0.4	238 (63)	178 (47)
Jet-milled	–	–	2900	1700

Particle size of the reference-milled samples is shown for comparison.

**Table III.** Volume- and Number-Weighted Mean Diameters and Corresponding Standard Deviations of Griseofulvin (GF) Particles Obtained Using the Continuous PSFEE at 50 g/min (CO<sub>2</sub>) and 5 ml/min (Emulsion) Flow Rates for Different Solvents, Surfactants, and Drug Concentrations

GF (% w/w)	Solvent content (% w/w)	Surfactant (% w/w water)	VMD (SD, in nm)	NMD (SD, in nm)
1	DCM (20)	Polyvinyl pyrrolidone (PVP)/1	545 (364)	–
0.8	DCM/20	Lecithin/2	760	224
1	EtAc/20	PVA/0.25	760	330
1	EtAc/20	PVP/1	978 (139)	784 (150)
Micronized, as supplied	–	–	5900	2300

Particle size of the reference-micronized sample is also shown for comparison.

important to note that there was no appreciable change on the solubility of MA or GF in water because of the presence of the surfactant. Negligible amount of MA (several parts per million) was detected in solution, whereas the dissolved GF in the above-mentioned nanosuspensions were about 20 ppm, which is a marginal increase from the solubility of GF in the buffer solution of 12 ppm (19).

## DISCUSSIONS

### Particle Formation in SFEE

Precipitation of nanoparticles in SFEE is brought about by the SC CO<sub>2</sub> extraction of the solvent from the emulsion phase. Although the detailed quantitative mechanism of this process has not yet been defined, the various stages of precipitation process are clear and can be illustrated in Figure 7. Each emulsion droplet may be considered as a “microreactor” where supersaturation, particle nucleation, and particle growth occur after the removal of organic phase. As soon as the emulsion is introduced into the SC CO<sub>2</sub> phase, the mass transfer of the organic solvent proceeds by two parallel pathways: (1) by direct extraction upon contact between SC CO<sub>2</sub> and the organic phase and (2) by diffusion of the organic solvent into water followed by consequent extraction of the solvent from the aqueous phase into SC CO<sub>2</sub>. There is also an inverse flux of CO<sub>2</sub> into the droplets leading to expansion of the organic phase and creating local supersaturation and precipitation of drugs. Although the solvents used to form the emulsions are considered to be “immiscible” with water, there is always a finite solubility in the aqueous phase. For example, toluene, dichloromethane, and ethyl acetate have solubilities in water of about 0.06, 0.6, and 10% w/w, respectively. This solubility may significantly

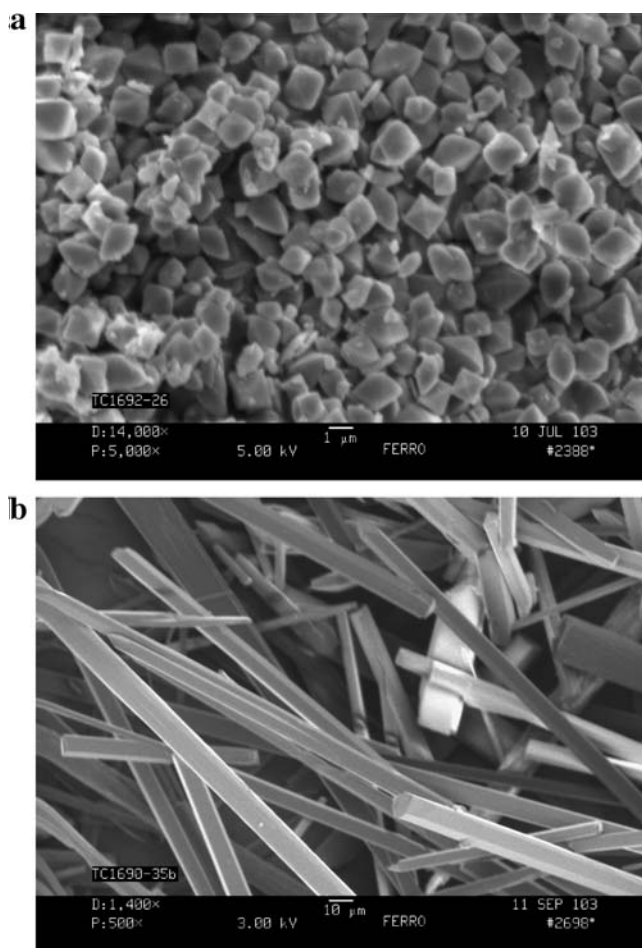


**Fig. 4.** (a) Morphology of the griseofulvin (GF) crystals produced using SFEE method [volume-weighted diameter (VMD) = 978 nm, number-weighted mean diameter (NMD) = 784 nm] in comparison with (b) crystals produced using supercritical antisolvent precipitation under the same conditions of pressure, temperature, and solution flow rate.

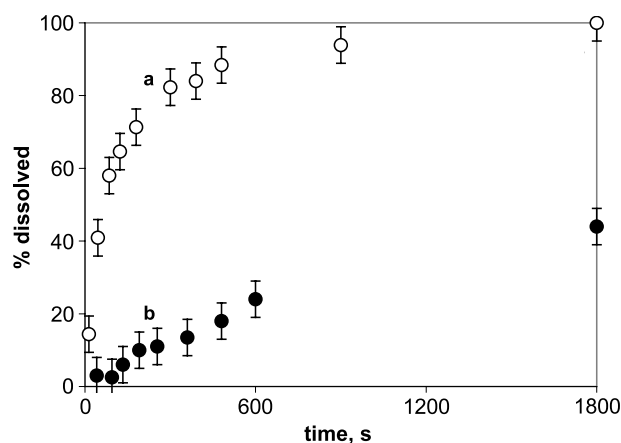


**Fig. 5.** Dissolution profile of megestrol acetate (MA) suspension with particles (a) VMD = 254 nm and NMD = 174 nm compared with (b) reference jet-milled material, with VMD = 2.9 μm and NMD = 1.7 μm.

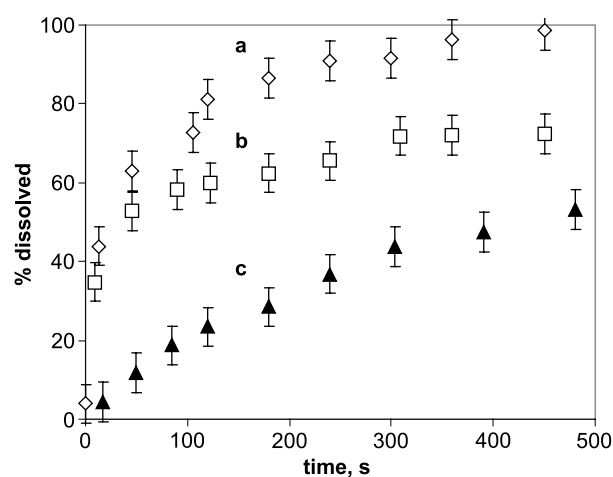


**Fig. 6.** Dissolution profiles of two GF suspensions with (a) VMD = 760 nm and NMD = 224 nm, and (b) VMD = 978 nm and NMD = 784 nm compared with a micronized material with (c) VMD = 5.9  $\mu\text{m}$  and NMD = 2.3  $\mu\text{m}$ .

increase the rate of mass transfer from the emulsion droplets into the aqueous phase. After the solvent extraction is completed, the nanoparticles remain in the aqueous phase, stabilized by the surfactant. The surfactant molecules present around the emulsion droplet act as protective layer and prevent particle growth by agglomeration. The size of particles produced is related to the emulsion droplet size and therefore depends on the stability of the emulsions. As a rule, finer and more stable emulsions produce nanosuspensions of smaller particle size and with narrower particle size distribution. However, the experiments with different materials show that this dependence may not be a direct proportionality between the emulsion droplet size and the particle size, as it would be expected for each droplet generating a single particle. For polymeric materials, such proportionality holds (19); however, for small molecule crystalline drugs, the particles produced are typically larger than the droplet size. Therefore, it can be assumed that particles formed in the internal emulsion phase undergo some interaction leading to particle growth. One of the reasons for such growth can be a small but significant solubility of the drug in the aqueous-organic phase during extraction. Increase of the organic phase may lead to a lower supersaturation furthering the particle growth. This phenomenon can explain the experimental dependences shown in Fig. 2.

The rate of extraction of the solvent from the emulsion droplet also has a significant effect on the size and the

morphology of the precipitated particles. Because solvent extraction efficiency from emulsions using SC  $\text{CO}_2$  is much higher than most of the well-known conventional methods such as evaporation, solvent extraction, and dilution, it provides for a faster precipitation route. Higher rates of extraction enable faster attainment of supersaturation, thus leading to the formation of greater number of nuclei and smaller and more uniform particles. It is observed that nanoparticles were successfully obtained from emulsions unstable under low pH conditions for GF nanoparticles prepared using emulsion with lecithin as surfactants. Therefore, it is likely that the rate of extraction is fast enough to cause precipitation before emulsion droplet agglomeration sets in causing phase separation. However, the precipitation within droplets occurs relatively slowly compared with a typical solution precipitation, providing the opportunity to attain thermodynamically stable crystalline structures.

There is a fundamental difference between the SFEE process and any antisolvent precipitation (supercritical or liquid) from a homogeneous solution. In the precipitation from solution, the particles are nucleated and grow within the whole solution volume. Therefore, the size of particles produced depends on the supersaturation during mixing and on the nucleation and growth constants, which are difficult to control (11). In the SFEE, the nucleation and growth are confined by the aqueous phase and therefore localized within the droplets, with some limited interaction between the droplets. As a result, the particle size obtained in SFEE is typically an order of magnitude smaller than those produced during solution precipitation.

Finally, SFEE is shown to be simpler, less bulky, and more efficient than most spray-drying or vacuum-drying equipment. The extraction column is made of inexpensive stainless-steel tubing, which produces a continuous flow of the product (suspensions) at a relatively large flow rate. Carbon dioxide is an inexpensive substance and can be recycled, if necessary, in an enclosed and economical process.

### Dissolution of Nanosuspensions

One of the main objectives of producing nanosuspensions is to increase the dissolution rate of drugs with poor aqueous solubility. It is therefore important to distinguish which physicochemical characteristics of these materials may contribute to the enhanced dissolution. Dissolution of a unit mass of solid,  $\text{dm}/(\text{mdt})$ , can be described by a general kinetic equation (Noyes–Witney) that was originally proposed for a dissolution or crystallization process controlled by diffusion. However, for poorly soluble substances, it has to be corrected by assuming the two consequent steps, the first-order process

**Table IV.** Dissolution Parameters for MA and GF Suspensions Obtained Using the Data in Figs. 5 and 6, Calculated Using Eqs. (1–4)

	MA(a)	MA(b)	GF(a)	GF(b)	GF(c)
$\text{dm}/(\text{mdt}), (\text{s}^{-1})$	$5.3 \times 10^{-3}$	$4.5 \times 10^{-4}$	$6.8 \times 10^{-3}$	$4.9 \times 10^{-3}$	$1.9 \times 10^{-3}$
SMD (m)	$0.21 \times 10^{-6}$	$2.3 \times 10^{-6}$	$0.6 \times 10^{-6}$	$0.88 \times 10^{-6}$	$4.1 \times 10^{-6}$
$c_0 (\text{kg m}^{-3})$	$2 \times 10^{-3}$	$2 \times 10^{-3}$	$12 \times 10^{-3}$	$12 \times 10^{-3}$	$12 \times 10^{-3}$
$S (\text{m}^2 \text{kg}^{-1})$	$2.15 \times 10^4$	$0.2 \times 10^4$	$0.77 \times 10^4$	$0.52 \times 10^4$	$0.11 \times 10^4$
$k_d (\text{m s}^{-1})$	$5.6 \times 10^{-3}$	$0.48 \times 10^{-3}$	$1.8 \times 10^{-3}$	$1.4 \times 10^{-3}$	$0.23 \times 10^{-3}$
$k (\text{m s}^{-1})$	$1.2 \times 10^{-4}$	$1.1 \times 10^{-4}$	$0.72 \times 10^{-4}$	$0.77 \times 10^{-4}$	$1.4 \times 10^{-4}$

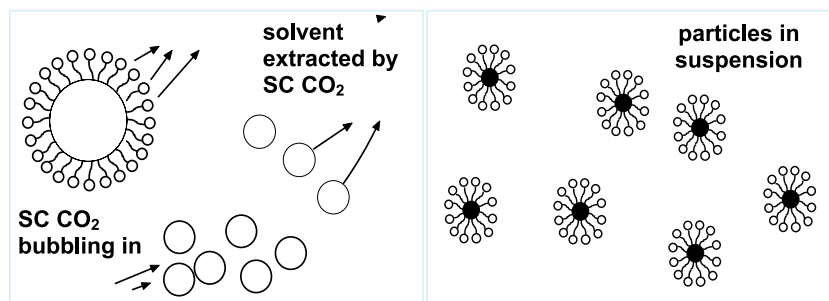


Fig. 7. Proposed mechanism of solvent extraction in the SFEE process.

of dissociation of molecules from the solid (crystal or amorphous) on the surface and the diffusion process from the surface to the solution bulk (20):

$$dm/(mdt) = kS(c_0 - c) \quad (1)$$

where  $c$  is the concentration of the drug in the bulk and  $c_0$  is the equilibrium concentration of the drug in solution (solubility). The total mass-transfer coefficient for dissolution  $k$  is defined by the diffusion  $k_d$  and surface kinetic  $k_s$  parts:

$$1/k = 1/k_d + 1/k_s \quad (2)$$

$$k_d = D/\delta \quad (3)$$

where the diffusion component is expressed through the effective thickness of the diffusion boundary layer  $\delta$  and the diffusion coefficient  $D$  of the drug in the aqueous media. The coefficient  $k_s$  is defined by the properties of the solid state and solution thermodynamics, whereas  $k_d$  is a function of the solution hydrodynamics (or stirring regime) and also of the particle size. For very small particles in a stagnant solution, the thickness  $\delta$  is approximately equal to the particle radius  $VMD/2$  (21). For well-stirred solution, the value of  $\delta$  may approach zero. The specific surface area can be calculated as:

$$S \approx 6/\rho \text{ (SMD)} \quad (4)$$

where  $\rho$  is the solid density and SMD is the surface-volume (Sauter) mean diameter that has an arbitrary value between NMD and VMD diameters.

There is also a phenomenon of increased equilibrium solubility for small particles, caused by the curvature of the particle-solution interface. This effect is defined by the Gibbs Eq. (20):

$$\ln(c_0^*/c_0) = 4\sigma V/(RT(VMD)) \quad (5)$$

where  $c_0^*$  is the adjusted solubility,  $c_0$  is the solubility with large particles ( $VMD > 1 \mu\text{m}$ ),  $\sigma$  is the interfacial tension,  $V$  is the molar volume,  $R$  is the gas constant,  $T$  is the absolute temperature, and  $\rho$  is the density of the solid.

Following the theoretical points given above, it is possible to calculate the most important dissolution parameters and to estimate the contribution of different factors. Firstly, using a typical magnitude of the interfacial tension,  $\sigma = 0.1 \text{ J/m}^2$ , it predicted that a characteristic shift of solubility for particles of 200 nm, according to Eq. (5), is

about 10%. Although this value is significant, it is not comparable with the increase of the specific surface area according to Eq. (4). Secondly, Eqs. (1)–(4) allow the numerical values of the dissolution coefficient  $k$  to be obtained using the experimental data from the initial slopes of the dissolution curves in Figs. 5 and 6 (Table IV). A good agreement, within 10%, is obtained for the kinetic coefficients measured for both MA and GF materials for crystalline materials of different particle size, with the exception of the amorphous sample GF(c). The amorphous compound should generally have a higher dissolution coefficient. Furthermore, it is clear that the value of  $k$  is at least an order of magnitude smaller than the predicted minimum diffusion mass-transfer coefficient  $k_d$  [calculated from Eq. (3) assuming a stagnant diffusion boundary layer with thickness  $\delta = VMD/2$ ]. Therefore, according to Eqs. (1) and (4), the dissolution process is mainly governed by the surface dissolution kinetics and the specific surface area, with lesser effects of the diffusion and thermodynamic equilibrium.

Finally, it should be noted that all materials produced using SFEE indicated a high degree of crystallinity. This compares favorably, in terms of the physical stability, with the amorphous materials often obtained by milling, solubilization, lyophilization, or rapid precipitation techniques. The aqueous nanosuspensions also indicated a high degree of stability with respect to particle size changes, which would likely be a result of the well-known Ostwald ripening effect. This effect can be quantified using the same Eq. (5), which shows the dependence of the drug solubility on the particle size. This solubility dependence results in the dissolution of finer particle fraction and growth of the coarser fraction. However, if the particle size is uniform, there is no driving force for such conversion. In addition, the surfactant adhered to particle surfaces may result in the reduction of the mass-transfer coefficient  $k$  and reduce the “ripening” effect. Decrease of the temperature should also lead to more stable suspensions, largely because the coefficient  $k$ , as all kinetic coefficients, should exhibit an Arrhenius-type exponential dependence on the temperature.

## CONCLUSION

The processing method SFEE reported in this work combines the advantages of emulsion methods, with their control of particle size, crystallinity, and surface properties with the continuous supercritical fluid extraction process,



which can offer an advanced chemical engineering and scale-up, higher product purity, and shorter processing times. This process, however, requires a careful formulation to provide the stable emulsion as well as stable particle suspension. The feasibility of the process was demonstrated for three different molecules. For pure drug molecules (i.e., without substantial addition of other additives such as lipids and polymers), the particles about 200 nm (volume mean diameter) were produced. It is likely that further size reduction can be achieved by means of formulation and optimization of the solvent system. The importance of fundamental mechanistic understanding is indicated. The dissolution of the nanosuspensions produced was analyzed in terms of the major kinetic and thermodynamic parameters. The results indicated that dissolution is governed mainly by the surface kinetic coefficient and the specific surface area of the particles.

#### ACKNOWLEDGMENTS

The authors thank Dave Gnizak and Sara Freeman, Ferro Analytical Department, for the SEM analysis and XRD studies, respectively. The authors also thank Dr. Carl Lentz for his advice during the design of the experimental studies.

#### REFERENCES

1. B. Sjostrom, B. Kronberg, and J. Carlfors. A method for preparation of submicron particles of sparingly water-soluble drugs by precipitation in oil-in-water emulsions. I: Influence of emulsification and surfactant concentration. *J. Pharm. Sci.* **82**:579–583 (1993).
2. C. Jacobs and R. H. Muller. Production and characterization of a budesonide nanosuspension for pulmonary administration. *Pharm. Res.* **19**:189–194 (2002).
3. B. E. Rabinow. Nanosuspensions in drug delivery. *Nat. Rev., Drug Discov.* **3**:785–796 (2004).
4. E. Merisko-Liversidge. Formulation and antitumor activity evaluation of nanocrystalline suspensions of poorly soluble anticancer drugs. *Pharm. Res.* **13**:272–278 (1996).
5. E. Merisko-Liversidge, G. G. Liversidge, and E. Cooper. Nano-sizing: a formulation approach for poorly water-soluble compounds. *Eur. J. Pharm. Sci.* **18**:113–120 (2003).
6. R. H. Muller and K. Peters. Nanosuspensions for the formulation of poorly water soluble drugs. I. Preparation by a size reductions technique. *Int. J. Pharm.* **160**:229–237 (1998).
7. M. Sarkari, J. Brown, X. Chen, S. Swinnea, R. O. Williams, and K. P. Johnston. Enhanced drug dissolution using evaporative precipitation into aqueous solution. *Int. J. Pharm.* **243**:17–31 (2002).
8. P. Bagchi, R. P. Scaringe, and H. W. Bosch. Coprecipitation of nanoparticulate pharmaceutical agents with crystal growth modifiers. U. S. Patent No. 5665331 (1997).
9. X. Chen, T. J. Young, M. Sarkari, R. O. Williams, and K. P. Johnston. Precipitation of cyclosporine A nanoparticles by evaporative precipitation into aqueous solutions. *Int. J. Pharm.* **242**:3–14 (2002).
10. B. Subramaniam, R. A. Rajewski, and K. Snavely. Pharmaceutical processing with supercritical carbon dioxide. *J. Pharm. Sci.* **86**:885–890 (1997).
11. J. Baldyga, M. Henczka, and B. Y. Shekunov. Fluid dynamics, mass-transfer and particle formation in supercritical fluids. In P. York, U.B. Kompella and B.Y. Shekunov (eds.), *Supercritical Fluid Technology for Drug Product Development. Drugs and the Pharmaceutical Sciences*, vol. 138, Marcel Dekker Series, New York, 2004, pp. 91–157.
12. J. Jung and M. Perrut. Particle design using supercritical fluids: literature and patent survey. *J. Supercrit. Fluids* **20**:179–219 (2001).
13. M. Trotta, M. Gallarate, M. E. Carlotti, and S. Morel. Preparation of griseofulvin nanoparticles from water-dilutable microemulsions. *Int. J. Pharm.* **254**:235–242 (2003).
14. M. Trotta, M. Gallarate, F. Pattarino, and S. Morel. Emulsions containing partially water-miscible solvents for the preparation of drug nanosuspensions. *J. Control. Release* **76**:119–128 (2001).
15. B. Sjostrom and B. Bergenstahl. Preparation of submicron drug particles in lecithin stabilized o/w emulsions. I. Model studies of the precipitation of cholesteryl acetate. *Int. J. Pharm.* **88**:53–62 (1992).
16. D. Kashchiev. *Nucleation: Basic Theory with Applications*, Butterworth-Heinemann, Oxford, 2000.
17. P. Chattopadhyay and R. B. Gupta. Production of griseofulvin nanoparticles using supercritical CO<sub>2</sub> antisolvent with enhanced mass transfer. *Int. J. Pharm.* **228**:19–31 (2001).
18. E. Reverchon and G. Della Porta. Production of antibiotic micro- and nano-particles by supercritical antisolvent precipitation. *Powder Technol.* **106**:23–29 (1999).
19. P. Chattopadhyay, B. Y. Shekunov, J. S. Seitzinger, and R. Huff. Particles from supercritical fluid extraction of emulsions (PSFEE): preparation of composite particles for drug targeting and controlled release. *AAPS PharmSci* **5**:W5099, 2003 (2003).
20. J. W. Mullin. *Crystallization*, 3rd Edn., Butterworth Heinemann, Oxford, 1993.
21. A. A. Chernov. *Modern Crystallography III, Crystal Growth*, Springer Series in Solid State Physics, Springer, Berlin, 1984.